Circulation: Cardiovascular Imaging

ORIGINAL ARTICLE

Impact of Coronary Lesion Geometry on Fractional Flow Reserve

Data From Interventional Cardiology Research In-Cooperation Society-Fractional Flow Reserve and Intravascular Ultrasound Registry

See Editorial by Hachamovitch

Do-Yoon Kang, MD*
Jung-Min Ahn, MD*
Young Woo Kim
Ji Young Moon, PhD
Joon Sang Lee, PhD
Bon-Kwon Koo, MD*
Pil Hyung Lee, MD
Duk-Woo Park, MD
Soo-Jin Kang, MD
Seung-Whan Lee, MD
Young-Hak Kim, MD
Seong-Wook Park, MD
Seung-Jung Park, MD*

BACKGROUND: The impact of various coronary lesion geometries on fractional flow reserve (FFR) is poorly understood.

METHODS AND RESULTS: A total of 1552 coronary lesions in 1236 patients from a prospective Interventional Cardiology Research In-cooperation Society Fractional Flow Reserve and Intravascular Ultrasound registry were assessed using quantitative coronary angiography, intravascular ultrasound, and FFR. Computational fluid dynamics simulation was performed for theoretical validation. Patients with complex geometries, such as longitudinal eccentricity, cross-sectional eccentricity, and surface roughness, showed significantly lower FFR values. In multivariable analysis, distal longitudinal eccentricity (adjusted odds ratio, 1.55; 95% confidence interval, 1.04–2.87; *P*=0.031), cross-sectional eccentricity (adjusted odds ratio, 1.65; 95% confidence interval, 1.27–2.14; *P*<0.001), and surface roughness (adjusted odds ratio, 1.55; 95% confidence interval, 1.04–2.32; *P*=0.033), as well as male sex, left anterior descending artery territory, proximal location, high degree of diameter stenosis, long lesion, and high plaque burden, were identified as independent predictors for significantly low FFR values (≤0.80). Computational simulation supported the impact of lesion geometry on FFR.

CONCLUSIONS: The complex coronary lesion geometries were independently associated with reduced FFR values. The visual–functional mismatch between coronary angiography and FFR could be partly attributable to local geometric factors.

CLINICAL TRIAL REGISTRATION: URL: https://www.clinicaltrials.gov. Unique identifier: NCT01366404.

*Drs Kang, Ahn, Koo, and Park contributed equally to this work.

Key Words: coronary angiography ■ coronary artery disease ■ cross-sectional studies ■ humans ■ registries

http://circimaging.ahajournals.org

CLINICAL PERSPECTIVE

Visual–functional mismatches between angiographic percentage diameter stenosis and fractional flow reserve (FFR) value are common, especially in intermediate stenosis. The degree of stenosis and the size of perfused myocardial mass were known to be the major determinants for FFR value. Previous studies have reported that the complex geometries of local lesions could be associated with lower FFR value. However, the impact of lesion geometries on FFR is poorly understood. The current study evaluated the impact of lesion-specific morphological characteristics of coronary stenoses on the FFR using quantitative coronary angiography, intravascular ultrasound, and FFR value from a prospective IRIS-FFR (Interventional Cardiology Research In-cooperation Society Fractional Flow Reserve) and intravascular ultrasound registry. The complex coronary lesion geometries of distal longitudinal eccentricity (an abrupt narrowing of the distal edge), cross-sectional eccentricity (asymmetrical narrowing in a cross-sectional view), surface roughness (irregular luminal surface) were identified as independent predictors for significantly low FFR values. Computational fluid dynamics simulation theoretically supported the findings. The results of this study suggest that the visual–functional mismatch between coronary angiography and FFR could be partly attributable to local geometric factors.

Coronary angiography visualizes the inner lumen of a vessel. Fractional flow reserve (FFR) value of ≤0.80 indicates the stenosis' potential to induce myocardial ischemia.[1,2] Therefore, FFR-guided diagnosis and revascularization for stable ischemic heart disease could be the gold standard in current practice. However, there are still many visual–functional mismatches between angiographic percentage diameter stenosis and FFR value especially in intermediate stenosis.[3]

The degree of stenosis and the size of perfused myocardial mass were the most important determinants for FFR value.[4,5] Although previous studies have reported that the complex geometries of local lesions, such as eccentricity, luminal irregularity, and plaque rupture, could be associated with lower FFR value,[3,6] the impact of lesion geometries on FFR is poorly understood (Figure 1).

For better understanding of the contribution of local geometric factors to the physiological effect of a stenosis, we investigated 1552 lesions using simultaneous FFR and intravascular ultrasound (IVUS) assessment from the prospective IRIS-FFR (Interventional Cardiology Research In-cooperation Society Fractional Flow Reserve) and IVUS registry. Computational fluid dynamics simulation was also performed for theoretical validation.

METHODS

The data, analytic methods, and study materials will be made available to other researchers for purposes of reproducing the results or replicating the procedure. The data that support the findings of this study are available from the corresponding author on reasonable request.

Patients and Lesion Characteristics

The IRIS-FFR registry was a prospective, multicenter study designed to investigate the natural history of coronary stenosis assessed by FFR in routine clinical practice. The registry consecutively enrolled all patients who underwent FFR measurement of at least 1 coronary lesion. Major exclusion criteria were left main artery lesions, TIMI (Thrombolysis In Myocardial Infarction) flow of <3, bypass graft, overt heart failure, and technical unsuitability for FFR evaluation.[7]

From August 2009 to October 2016, 10 881 lesions from 7735 patients were prospectively enrolled, of which 1552 nonleft main coronary lesions in 1236 patients were assessed using simultaneous FFR and IVUS. The decision to conduct an IVUS measurement was at the discretion of the operator. The study protocol was approved by the institutional review board or ethical committee at each participating center, and all subjects provided written informed consent.

FFR Measurement

FFR was measured using a commercially available coronary pressure wire as previously described.[7] After administration of intracoronary nitrate (100 or 200 µg), the pressure wire was positioned at the distal segment of the target lesion. Intravenous adenosine infusion via the central vein or large antecubital vein was recommended as the standard method to induce coronary hyperemia. The hyperemic proximal aortic pressure and the distal arterial pressure were measured during sustained hyperemia, and the FFR value was calculated as the mean distal arterial pressure/proximal aortic pressure during hyperemia.

Quantitative and Qualitative Coronary Angiography

Quantitative coronary angiography was performed using standard techniques with automated edge-detection algorithms (CAAS-5; Pie-Medical, Maastricht, the Netherlands). Angiographic percentage diameter stenosis, minimal lumen diameter, lesion length, and reference lumen diameter were measured.[8] Surface roughness was defined as an irregular luminal surface by intraluminal calcification, intimal flap, or sawtooth pattern. Lesions with a small crater consisting of a discrete luminal widening around the stenosis with consistent IVUS finding were classified as plaque rupture.[9]

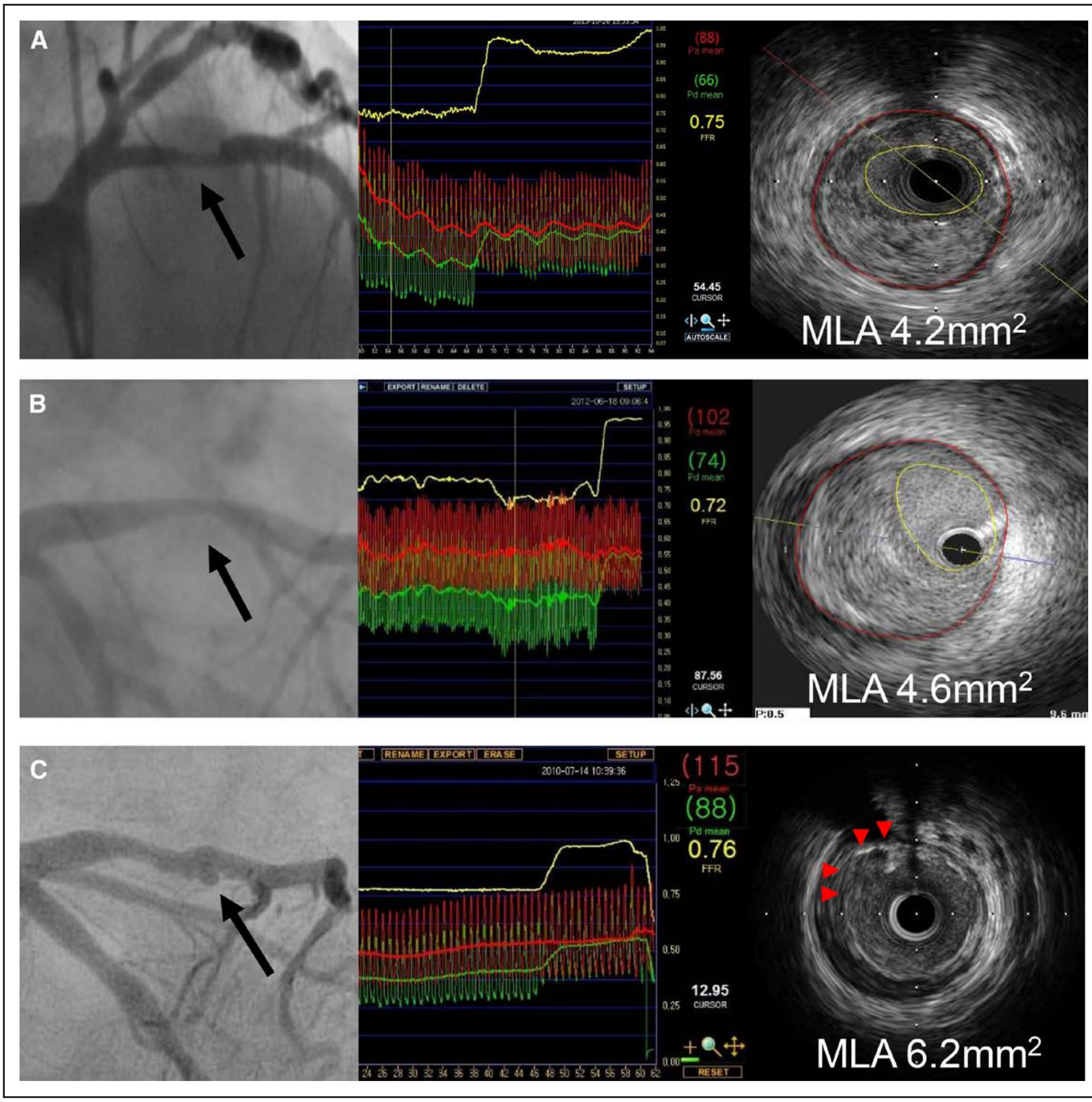

Figure 1. Examples of complex lesion geometries.
A, A 62-y-old man with stable angina. Angiographic DS was 40% with longitudinal eccentricity (black **arrow**), and intravascular ultrasound-minimal lumen area (IVUS-MLA) was 4.2 mm^2, whereas fractional flow reserve (FFR) was 0.75 (reverse mismatch). **B**, A 58-y-old man with stable angina. Angiographic DS was 50% with cross-sectional eccentricity (black **arrow**), and IVUS-MLA was 4.6 mm^2. FFR was reduced to 0.72 (reverse mismatch). **C**, A 68-y-old man with unstable angina. Angiographic DS was only 30% with plaque rupture. IVUS showed MLA 6.2 mm^2 and ruptured plaque (red **arrow**). FFR was reduced to 0.76 (reverse mismatch). DS indicates diameter stenosis.

Intravascular Ultrasound

IVUS imaging was performed using a commercial scanner (Boston Scientific Scimed, Inc, Minneapolis, MN or Volcano Therapeutics, Rancho Cordova, CA) with a rotating, 40 MHz transducer within a 3.2Fimaging sheath while pulling back the transducer at 0.5 mm/s. Using computerized planimetry (EchoPlaque 3.0; Indec Systems, Mountain View, CA), offline quantitative IVUS analysis was performed in accordance with standard methods.[10] Minimal lumen area and external elastic membrane area at the minimal lumen area site were measured. The plaque plus media area was calculated as external elastic membrane−lumen area. Plaque burden was calculated as (plaque+media)/external elastic membrane×100 (%).

Longitudinal eccentricity (LE) was defined as stenosis with an abrupt narrowing of the proximal or distal edge (Figure 2). The LE index was defined as the ratio of distance (x) between the proximal end of the lesion and the site of minimal lumen area to the lesion length (L). The lesion with LE ≤0.25 was classified with proximal LE while LE ≥0.75 with distal LE. Cross-sectional eccentricity (CE) index was defined as the ratio of maximum to minimum plaque plus media thickness at the site of minimal lumen area. Lesions with CE index >3 was set to have CE (Figure 2).[11] IVUS and quantitative coronary angiography were analyzed in the core laboratory of the CardioVascular Research Foundation (Seoul, Korea).

Computational Fluid Dynamics: Numeric Methods

Computational fluid dynamics simulation was performed for theoretical validation of the impact of lesion geometry

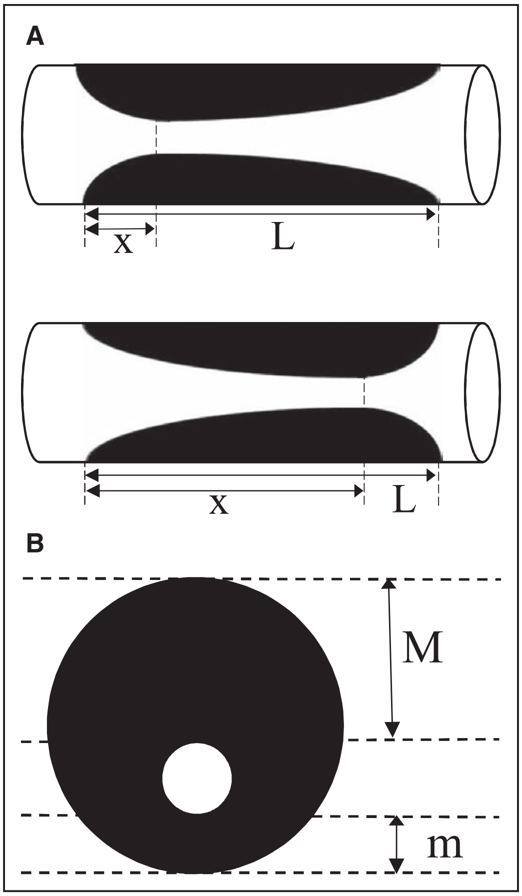

Figure 2. The definition of longitudinal eccentricity (LE) and cross-sectional eccentricity (CE).
A, The LE index was defined as the ratio of distance (x) between the proximal end of the lesion and the site of minimal lumen area to the lesion length (L). The lesion with LE ≤0.25 was classified with proximal LE while LE ≥0.75 with distal LE. **B**, CE index was defined as the ratio of maximum to minimum plaque plus media thickness at the site of minimal lumen area (M/m). Lesions with CE index >3 was set to have a CE.

on FFR. The lattice Boltzmann method with the single-time Bhatnagar–Gross–Krook model was used for blood flow simulation.[12–14] The blood velocity in the vessel was described using the pulsatile flow condition, and the prescribed velocity was used at the inlet.[15] The frequency of the pulsatile flow was set to once per second, similar with the normal heart rate. The velocity at peak pulsatile flow was set to 0.5 m/s. For the outlet boundary, impedance boundary condition was used to analyze the reflected pressure wave by the viscoelasticity of the blood vessel.[16] The flow was assumed to be hyperemic to make similar conditions with that of clinical invasive FFR measurement. The blood density was fixed at 1080 kg/m^3. The Carreau model $(\mu-\mu_\infty)/(\mu_0-\mu_\infty)=\left[1+(\lambda\gamma)^2\right]^{(n-1)/2}$ was used for non-Newtonian characterization of blood, and the following parameters were used: $\mu_0=0.056\text{Pa}\times\text{s}$, $\mu_\infty=0.0035\ \text{Pa}\times\text{s}$, n=0.3568, and λ=3.313s.[17] Blood vessel diameter for all cases was 3 mm, and the length was 21 mm. To focus on the geometric factor of a stenosis, the blood vessel was assumed to be a rigid wall. No-slip boundary condition was used for the vessel wall. The FFR value was calculated using the average pressure 6 mm away from the lesion in the upstream direction and 9 mm in the downstream direction.

Table 1. Clinical Characteristics of 1236 Patient

Parameters	All (n=1236)
Age, y	63.6±9.5
Sex, male, n (%)	896 (72.5)
Body mass index, kg/m^2	25.0±2.8
Hypertension, n (%)	787 (63.7)
Diabetes mellitus, n (%)	354 (28.6)
Dyslipidemia, n (%)	966 (78.2)
Current smoking, n (%)	299 (24.2)
Previous percutaneous coronary intervention, n (%)	202 (16.3)
Previous myocardial infarction, n (%)	63 (5.1)
Previous stroke, n (%)	60 (4.9)
Clinical manifestation, n (%)	
Stable angina	635 (51.4)
Unstable angina	188 (15.2)
Non–ST-segment–elevation myocardial infarction	68 (5.5)
Silent ischemia	345 (27.9)

The vortex structure model was used to explain the impact of lesion geometries on FFR. Vortex is a swirling flow of blood developed beyond the stenosis. Vortex length, which is the length between the separation point and the point at which the streamline attaches to the vessel— the velocity gradient is zero— is used to quantify the vortex structure (Figure IA in the Data Supplement).

Statistical Analysis

Continuous variables are expressed as mean±SD; categorical variables are expressed as counts and percentages. Continuous variables were compared using unpaired *t* tests and categorical variables using the χ^2 test. Baseline variables that showed a univariate relationship (P<0.05) with the FFR value were entered into multivariable logistic regression models to find predictors of significantly low FFR (≤0.80). Variables for inclusion were carefully chosen, given the number of events available, to ensure parsimony of the final models, and nonsignificant variables were excluded by backward selection. The multiple lesions within a patient were considered to be independent. All statistical analyses were performed using SPSS version 21.0 (IBM Corporation, Armonk, NY) and R version 3.2.3 (R Foundation for Statistical Computing, Vienna, Austria). *P* values were considered statistically significant if <0.05.

RESULTS

Impact of Lesion Geometries on the FFR Value

A total of 1236 patients with 1552 nonleft main de novo coronary lesions were enrolled. The mean age was 64 years, 73% of the patients were men, and 29% were diabetic. The average FFR value was 0.82, and 50.3% lesions showed significantly reduced FFR value (≤0.80).

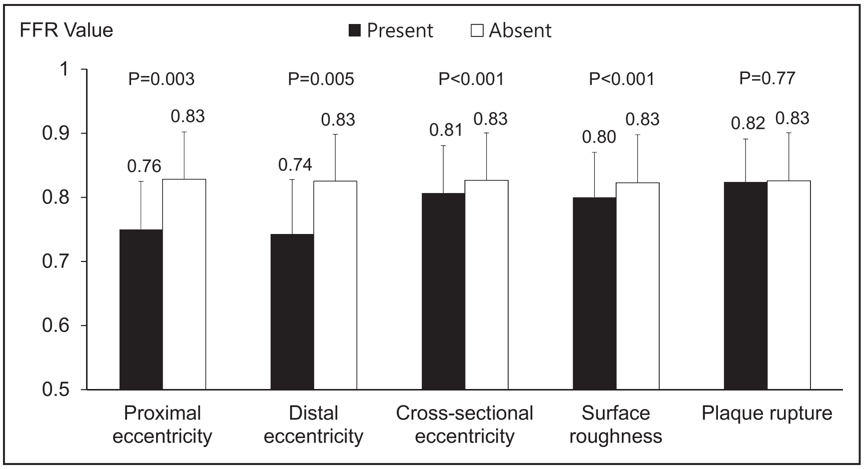

Figure 3. Fractional flow reserve (FFR) value according to the presence of complex lesion geometry.

Lesions with FFR values ≤0.80 showed higher diameter stenosis (53.5%±10.7% versus 46.5%±10.0%; *P*<0.001), smaller minimal lumen diameter (1.4±0.3 versus 1.7±0.4 mm; *P*<0.001), and longer lesion length (21.1±11.2 versus 16.1±9.0 mm; *P*<0.001) on quantitative coronary angiography analysis and small-

Table 2. Angiographic and IVUS Parameters of 1552 Lesions

Parameters	All (n=1552)	FFR ≤0.80 (n=782)	FFR >0.80 (n=770)	*P* Value
Lesion territory, n (%)				<0.001
Left anterior descending artery	1053 (67.8)	631 (80.7)	422 (54.8)	
Left circumflex artery	90 (5.8)	42 (5.4)	48 (6.2)	
Right coronary artery	409 (26.4)	109 (13.9)	300 (39.0)	
Lesion location, n (%)				0.002
Proximal	835 (53.8)	449 (57.4)	386 (50.1)	
Mid	601 (38.7)	273 (34.9)	328 (42.6)	
Distal	116 (7.5)	60 (7.7)	56 (7.3)	
Fractional flow reserve	0.82±0.07	0.76±0.05	0.88±0.05	<0.001
Quantitative coronary angiography				
Lesion length, mm	18.6±10.4	21.1±11.2	16.1±9.0	<0.001
Reference lumen diameter, mm	3.2±0.6	3.1±0.5	3.3±0.2	<0.001
Minimal lumen diameter, mm	1.6±0.4	1.4±0.3	1.7±0.4	<0.001
Diameter stenosis, %	50.1±11.0	53.5±10.7	46.5±10.0	<0.001
Diameter stenosis >50%, n (%)	770 (49.6)	486 (62.1)	296 (37.9)	<0.001
≤40%	299 (19.3)	90 (11.5)	209 (27.1)	<0.001
41%–50%	483 (31.1)	206 (26.3)	277 (36.0)	
51%–60%	523 (33.7)	288 (36.8)	235 (30.5)	
≥60%	247 (15.9)	198 (25.3)	49 (6.4)	
Surface roughness, n (%)	153 (9.9)	90 (11.5)	63 (8.2)	0.028
Intravascular ultrasound				
Lesion length, mm	31.8±13.8	30.7±14.0	32.9±13.6	0.002
External elastic membrane area, mm^2	12.1±4.8	12.2±4.9	12.0±4.6	0.47
Minimal lumen area, mm^2	3.0±1.3	2.9±1.3	3.0±1.4	0.09
Plaque plus media area, mm^2	9.1±4.2	9.2±4.4	8.9±4.0	0.18
Plaque burden, %	41.0±24.2	42.7±25.2	39.3±23.1	0.006
Plaque burden ≥70%, n (%)	342 (22.1)	197 (25.2)	145 (18.8)	0.002
Proximal longitudinal eccentricity, n (%)	141 (9.1)	92 (11.8)	49 (6.4)	<0.001
Distal longitudinal eccentricity, n (%)	118 (7.6)	85 (10.9)	33 (4.3)	<0.001
Cross-sectional eccentricity, n (%)	511 (32.9)	208 (26.6)	303 (39.4)	<0.001
Plaque rupture, n (%)	216 (13.9)	113 (14.5)	103 (13.4)	0.22

FFR indicates fractional flow reserve; and IVUS, intravascular ultrasound.

Table 3. Predictors of FFR ≤0.80 by Logistic Regression Models

	Univariable Analysis			Multivariable Analysis*		
Parameters	**OR**	**95% CI**	***P* Value**	**Adjusted OR**	**95% CI**	***P* Value**
Age ≥64 y	1.12	0.92–1.37	0.258			
Male sex	1.73	1.38–2.18	<0.001	2.22	1.69–2.93	<0.001
Diabetes mellitus	1.05	0.84–1.30	0.676			
Hypertension	1.07	0.87–1.31	0.549			
Left anterior descending artery	3.44	2.74–4.32	<0.001	3.62	2.77–4.72	<0.001
Left circumflex artery	0.85	0.56–1.31	0.467			
Right coronary artery	0.25	0.20–0.33	<0.001			
Proximal location	1.35	1.10–1.64	0.004	1.93	1.50–2.49	<0.001
QCA parameters						
Lesion length ≥16 mm	2.30	1.87–2.81	<0.001	2.14	1.68–2.71	<0.001
Minimal lumen diameter ≤1.5 mm	3.99	3.23–4.94	<0.001			
Diameter stenosis ≤40%	1	Reference	…	1	Reference	…
41%–50%				2.62	1.82–3.78	<0.001
51%–60%				4.12	2.81–6.05	<0.001
>60%				10.84	6.93–19.94	<0.001
Surface roughness	1.46	1.04–2.05	0.029	1.55	1.04–2.32	0.033
IVUS parameters						
Minimal lumen area ≤2.75 mm^2	1.08	0.88–1.31	0.48			
Plaque burden ≥70%	1.45	1.14–1.85	0.002	1.32	0.99–1.77	0.063
Proximal longitudinal eccentricity	1.96	1.37–2.82	<0.001			
Distal longitudinal eccentricity	2.72	1.80–4.13	<0.001	1.55	1.04–2.87	0.031
Cross-sectional eccentricity	1.72	1.39–2.13	<0.001	1.65	1.27–2.14	<0.001
Plaque rupture	1.20	0.90–1.61	0.22			

CI indicates confidence interval; FFR, fractional flow reserve; IVUS, intravascular ultrasound; OR, odds ratio; and QCA, quantitative coronary angiography.

*Adjusted by multivariable logistic regression analysis with sex, lesion territory, lesion location, diameter stenosis, lesion length, surface roughness, plaque burden, distal longitudinal eccentricity, and cross-sectional eccentricity.

er minimal lumen area (2.9±1.3 versus 3.1±1.4 mm^2; *P*=0.082) and higher plaque burden (42.6%±25.2% versus 39.3%±23.1%; *P*=0.007) on IVUS analysis (Tables 1 and 2).

Male sex, left anterior descending artery location of the lesion, high degree of diameter stenosis, lesion length ≥16 mm, plaque burden ≥70%, LE and CE, and surface roughness were more prevalent in patients with FFR values ≤0.80 by univariate analysis. Multivariable analysis identified that complex lesion geometries, such as distal LE, CE, and surface roughness, as well as male sex, left anterior descending artery territory, proximal location, high degree of diameter stenosis, lesion length of ≥16 mm, and plaque burden ≥70%, were independent predictors for significantly low FFR (Figure 3; Table 3).

Explanatory Computational Fluid Dynamics Simulation

Computational dynamic simulation study was performed in cases of different lesion geometries with LE, CE, surface roughness, and the presence of plaque rupture. The simulation study clearly demonstrated that the increased distal LE, CE, and surface roughness decreased FFR value (Figure 4).

DISCUSSION

In the present study, we found that complex coronary lesion geometries with distal LE, CE, and surface roughness independently affected the FFR value. This could explain the visual–functional mismatch—angiographically tight stenosis with negative FFR and insignificant stenosis with positive FFR—between coronary angiography and FFR.[4,18–20]

There have been limited studies using simultaneous coronary imaging and physiology. To the best of our knowledge, this prospective study is the first to simultaneously assess FFR, IVUS, and coronary angiography to evaluate the impact of coronary lesion-specific geometries on its functional significance.

A subgroup analysis of the FAME trial (Fractional Flow Reserve versus Angiography for Multivessel Evaluation) showed that 65% of coronary lesions with 50%

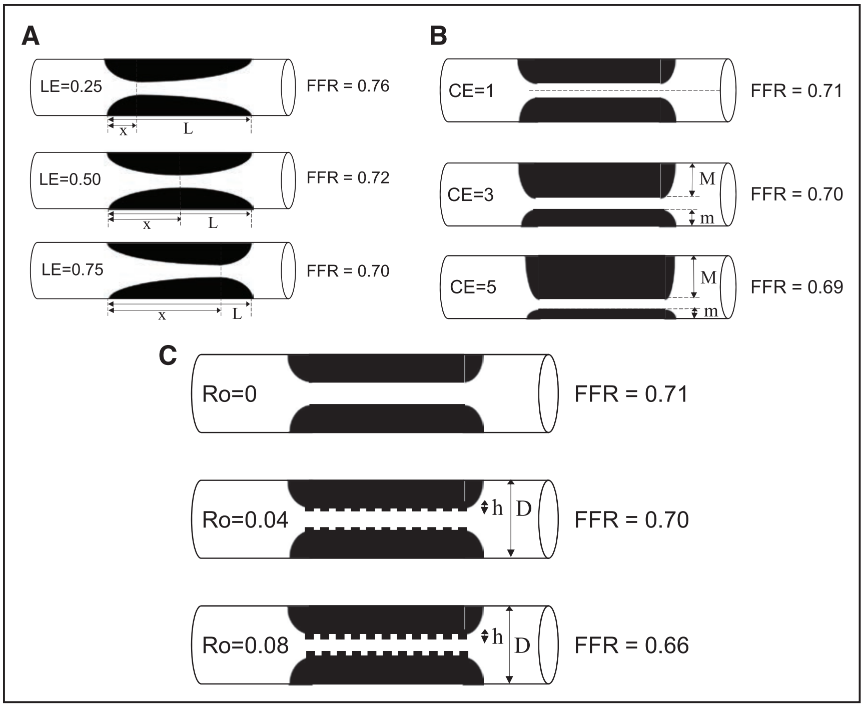

Figure 4. The fractional flow reserve (FFR) by computational fluid dynamics simulation according to various lesion geometries with 70% of diameter stenosis.
A, Longitudinal eccentricity (LE) was defined as x/L. **B**, Cross-sectional eccentricity (CE) was defined as M/m. **C**, Surface roughness. RO was defined as h/D (h was the height of the bumps at the lesion surface, D was vessel diameter).

to 70% diameter stenosis was functionally insignificant. Even in more severe stenoses with 71% to 90% diameter, 20% of the lesions did not show functional significance.[18] A few pilot studies showed that lesion factors, such as the degree of stenosis, lesion length, and various geometries, were associated with FFR.[6,17,21]

Computational simulation studies provided important insight to better understand the visual–functional mismatch. That is, even in the same degree of stenosis, different lesion geometry can make a different FFR value. The impact of lesion geometry on FFR value can be explained by the vortex structure. Energy loss of blood flow by vortex results in decreased FFR value, and longer vortex length after stenosis indicates larger energy loss. The vortex length became longer according to the different geometric simulation, such as distal LE, CE, and surface roughness even in the same degree of stenosis, which resulted in lower FFR. Figure IB in the Data Supplement visualized the increased vortex length by the degree of LE.

Therefore, the results of clinical and simulation study provide further insight on the reason why there are so many mismatches between angiographic diameter stenosis and FFR. The visual–functional mismatch between coronary angiography and FFR could be attributable to these lesion-specific geometric factors on top of the size of perfused myocardial mass and the degree of stenosis. Consideration of local geometry will improve understanding of the functional status of coronary artery disease. Further study is warranted to investigate the clinical impact of the lesion geometries.

Previous smaller studies reported that plaque rupture was associated with reduced FFR,[4,22] whereas plaque rupture was not associated with reduced FFR in this study. In simulation, narrow and deep rupture was associated with reduced FFR by additional vortex inside rupture whereas wide rupture was not (Figure II in the Data Supplement). Overall number of ruptures was limited, so larger studies will be necessary to evaluate the impact of plaque rupture on FFR.

This study has several limitations. First, there is the inherent limitation of observational registry study. Because FFR and IVUS evaluation was at discretion of operator, this might introduce selection bias (Tables I and II in the Data Supplement). Second, FFR measurement was not reviewed in core laboratory. Third, in the simulation study, the vessel was assumed to be a rigid wall.

CONCLUSIONS

The coronary lesion geometries of distal LE, CE, and surface roughness were independently associated with reduced FFR value. The visual–functional mismatch between coronary angiography and FFR could be partly attributable to lesion-specific geometric factors.

ARTICLE INFORMATION

Received August 27, 2017; accepted April 25, 2018.
The Data Supplement is available at http://circimaging.ahajournals.org/lookup/suppl/doi:10.1161/CIRCIMAGING.117.007087/-/DC1.

Affiliations

Heart Institute, Asan Medical Center, University of Ulsan College of Medicine, Seoul, South Korea (D.-Y.K., J.-M.A., P.H.L., D.-W.P., S.-J.K., S.-W.L., Y.-H.K., S.-W.P., S.-J.P.). School of Mechanical Engineering, Yonsei University, Seoul, South

Korea (Y.W.K., J.S.L.). School of Aerospace, Mechanical, and Mechatronic Engineering, The University of Sydney, Australia (J.Y.M.). Department of Internal Medicine and the Cardiovascular Center, Seoul National University Hospital, South Korea (B.-K.K.).

Sources of Funding

This study was supported by the CardioVascular Research Foundation and the grant 2015–7007 from the Asan Institute for Life Sciences, Seoul, Korea.

Disclosures

None.

REFERENCES

1. Pijls NH, De Bruyne B, Peels K, Van Der Voort PH, Bonnier HJ, Bartunek J Koolen JJ, Koolen JJ. Measurement of fractional flow reserve to assess the functional severity of coronary-artery stenoses. *N Engl J Med*. 1996;334:1703–1708. doi: 10.1056/NEJM199606273342604.
2. De Bruyne B, Fearon WF, Pijls NH, Barbato E, Tonino P, Piroth Z, Jagic N, Mobius-Winckler S, Rioufol G, Witt N, Kala P, MacCarthy P, Engström T, Oldroyd K, Mavromatis K, Manoharan G, Verlee P, Frobert O, Curzen N, Johnson JB, Limacher A, Nüesch E, Jüni P; FAME 2 Trial Investigators. Fractional flow reserve-guided PCI for stable coronary artery disease. *N Engl J Med*. 2014;371:1208–1217. doi: 10.1056/NEJMoa1408758.
3. Park SJ, Kang SJ, Ahn JM, Shim EB, Kim YT, Yun SC, Song H, Lee JY, Kim WJ, Park DW, Lee SW, Kim YH, Lee CW, Mintz GS, Park SW. Visual-functional mismatch between coronary angiography and fractional flow reserve. *JACC Cardiovasc Interv*. 2012;5:1029–1036. doi: 10.1016/j.jcin.2012.07.007.
4. Cho HO, Nam CW, Cho YK, Yoon HJ, Park HS, Kim H, Chung IS, Doh JH, Koo BK, Hyun DW, Hur SH, Kim YN, Kim KB. Characteristics of function-anatomy mismatch in patients with coronary artery disease. *Korean Circ J*. 2014;44:394–399. doi: 10.4070/kcj.2014.44.6.394.
5. Leone AM, De Caterina AR, Basile E, Gardi A, Laezza D, Mazzari MA, Mongiardo R, Kharbanda R, Cuculi F, Porto I, Niccoli G, Burzotta F, Trani C, Banning AP, Rebuzzi AG, Crea F. Influence of the amount of myocardium subtended by a stenosis on fractional flow reserve. *Circ Cardiovasc Interv*. 2013;6:29–36. doi: 10.1161/CIRCINTERVENTIONS.112.971101.
6. Takashima H, Waseda K, Gosho M, Kurita A, Ando H, Sakurai S, Maeda K, Kumagai S, Suzuki A, Amano T. Severity of morphological lesion complexity affects fractional flow reserve in intermediate coronary stenosis. *J Cardiol*. 2015;66:239–245.
7. Ahn JM, Park DW, Shin ES, Koo BK, Nam CW, Doh JH, Kim JH, Chae IH, Yoon JH, Her SH, Seung KB, Chung WY, Yoo SY, Lee JB, Choi SW, Park K, Hong TJ, Lee SY, Han M, Lee PH, Kang SJ, Lee SW, Kim YH, Lee CW, Park SW, Park SJ; IRIS-FFR Investigators†. Fractional flow reserve and cardiac events in coronary artery disease: data from a prospective IRIS-FFR registry (Interventional Cardiology Research Incooperation Society Fractional Flow Reserve). *Circulation*. 2017;135:2241–2251. doi: 10.1161/CIRCULATIONAHA.116.024433.
8. Ryan TJ, Faxon DP, Gunnar RM, Kennedy JW, King SB 3rd, Loop FD, Peterson KL, Reeves TJ, Williams DO, Winters WL Jr. Guidelines for percutaneous transluminal coronary angioplasty. a report of the American College of Cardiology/American Heart Association Task Force on Assessment of Diagnostic and Therapeutic Cardiovascular Procedures (Subcommittee on Percutaneous Transluminal Coronary Angioplasty). *Circulation*. 1988;78:486–502.
9. Popma JT, Almonacid A, Burke D. Qualitative and quantitative coronary angiography. In: Topol EJ, ed, *Textbook of Interventional Cardiology*. 6th ed. Philadelphia, PA: W.B. Saunders; 2011:757–775.
10. Mintz GS, Nissen SE, Anderson WD, Bailey SR, Erbel R, Fitzgerald PJ, Pinto FJ, Rosenfield K, Siegel RJ, Tuzcu EM, Yock PG. American College of Cardiology Clinical Expert Consensus Document on standards for acquisition, measurement and reporting of intravascular ultrasound studies (IVUS). A report of the American College of Cardiology Task Force on Clinical Expert Consensus Documents. *J Am Coll Cardiol*. 2001;37:1478–1492.
11. Mintz GS, Popma JJ, Pichard AD, Kent KM, Satler LF, Chuang YC, DeFalco RA, Leon MB. Limitations of angiography in the assessment of plaque distribution in coronary artery disease: a systematic study of target lesion eccentricity in 1446 lesions. *Circulation*. 1996;93:924–931.
12. Kim YW, Moon JY, Cho KR, Lee JS. Impedance boundary condition analysis of aging-induced wave reflections in blood flow. *Korea-Austr Rheol J*. 2013;25: 217–225.
13. Farhat H, Lee JS, Kondaraju S. *Accelerated Lattice Boltzmann Model for Colloidal Suspensions*. London, United Kingdom: Springer; 2014:346.
14. Moon JY, Suh DC, Lee YS, Kim YW, Lee JS. Considerations of blood properties, outlet boundary conditions and energy loss approaches in computational fluid dynamics modeling. *Neurointervention*. 2014;9:1–8. doi: 10.5469/neuroint.2014.9.1.1.
15. Zou Q, He X. On pressure and velocity boundary conditions for the lattice Boltzmann BGK model. *Physics of Fluids* 1997; 9:1591–1598.
16. Itu LM, Suciu C, Postelnicu A, Moldoveanu F. Analysis of outflow boundary condition implementations for 1D blood flow models. E-Health and Bioengineering Conference (EHB), Iasi, Romania: IEEE; 2011:1–4.
17. Jaffe R, Halon DA, Roguin A, Rubinshtein R, Lewis BS. A Poiseuille-based coronary angiographic index for prediction of fractional flow reserve. *Int J Cardiol*. 2013;167:862–865. doi: 10.1016/j.ijcard.2012.01.100.
18. Tonino PA, Fearon WF, De Bruyne B, Oldroyd KG, Leesar MA, Ver Lee PN, Maccarthy PA, Van't Veer M, Pijls NH. Angiographic versus functional severity of coronary artery stenoses in the FAME study fractional flow reserve versus angiography in multivessel evaluation. *J Am Coll Cardiol*. 2010;55:2816–2821. doi: 10.1016/j.jacc.2009.11.096.
19. Toth G, Hamilos M, Pyxaras S, Mangiacapra F, Nelis O, De Vroey F, Di Serafino L, Muller O, Van Mieghem C, Wyffels E, Heyndrickx GR, Bartunek J, Vanderheyden M, Barbato E, Wijns W, De Bruyne B. Evolving concepts of angiogram: fractional flow reserve discordances in 4000 coronary stenoses. *Eur Heart J*. 2014;35:2831–2838. doi: 10.1093/eurheartj/ehu094.
20. Christou MA, Siontis GC, Katritsis DG, Ioannidis JP. Meta-analysis of fractional flow reserve versus quantitative coronary angiography and noninvasive imaging for evaluation of myocardial ischemia. *Am J Cardiol*. 2007;99:450–456. doi: 10.1016/j.amjcard.2006.09.092.
21. López-Palop R, Carrillo P, Cordero A, Frutos A, Mateo I, Mashlab S, Roldán J. Effect of lesion length on functional significance of intermediate long coronary lesions. *Catheter Cardiovasc Interv*. 2013;81:E186–E194. doi: 10.1002/ccd.24459.
22. Kang SJ, Lee JY, Ahn JM, Song HG, Kim WJ, Park DW, Yun SC, Lee SW, Kim YH, Mintz GS, Lee CW, Park SW, Park SJ. Intravascular ultrasound-derived predictors for fractional flow reserve in intermediate left main disease. *JACC Cardiovasc Interv*. 2011;4:1168–1174. doi: 10.1016/j.jcin.2011.08.009.